Detailed Kinetic Study of the Growth of Small Polycyclic Aromatic Hydrocarbons. 1. 1-Naphthyl + Ethyne†

ARTICLE *in* THE JOURNAL OF PHYSICAL CHEMISTRY A · DECEMBER 2000

Impact Factor: 2.69 · DOI: 10.1021/jp002428q

6 AUTHORS, INCLUDING:

Henning Richter
Independent Researcher
56 PUBLICATIONS **2,031** CITATIONS
SEE PROFILE

Joseph W. Bozzelli
New Jersey Institute of Technology
277 PUBLICATIONS **5,260** CITATIONS
SEE PROFILE

Detailed Kinetic Study of the Growth of Small Polycyclic Aromatic Hydrocarbons. 1. 1-Naphthyl + Ethyne†

Henning Richter,‡ Oleg A. Mazyar,‡ Raman Sumathi,‡ William H. Green,*,‡ Jack B. Howard,‡ and Joseph W. Bozzelli§

Department of Chemical Engineering, Massachusetts Institute of Technology, 77 Massachusetts Avenue, Cambridge, Massachusetts 02139-4307, and Department of Chemical Engineering, Chemistry & Environmental Science, New Jersey Institute of Technology, Newark, New Jersey 07102

Received: July 7, 2000; In Final Form: October 18, 2000

A better understanding of the formation of polycyclic aromatic hydrocarbons (PAH) is of great practical interest because of their potential hazardous health effects and their role as intermediates in soot and fullerene formation. The potential surfaces of the reactions $C_6H_5 + C_2H_2$ and $1\text{-}C_{10}H_7 + C_2H_2$ were explored by density-functional theory using BLYP and B3LYP functionals. Vibrational analysis allowed the determination of thermodynamic data and deduction of high-pressure-limit rate constants via transition state theory. The pressure and temperature dependences of these chemically activated reactions were computed using the modified strong collision approximation. The comparison of the predictions for the $C_6H_5 + C_2H_2$ system with experimental data showed good agreement in particular at high temperatures relevant for a combustion environment. The dominant product from acetylene addition to 1-naphthyl at low pressures is the five-membered ring species acenaphthylene, consistent with the more pronounced formation of fullerenes under such conditions. High pressure favors formation of stabilized initial adducts, i.e., phenylvinyl and 1-naphthylvinyl. Some products not considered previously, such as 1-acenaphthenyl, 1-naphthylacetylene, 2-vinylphenyl, and 1-vinyl-2-phenyl, are found to be important under some pressure and temperature conditions. All of our results are consistent with known free-radical chemistry. Rate constants describing the formation of phenylacetylene, phenylvinyl, 1-vinyl-2-phenyl, 1-naphthylvinyl, 1-vinyl-8-naphthyl, 1-naphthylacetylene, acenaphthylene, and 1-acenaphthenyl are given at 20 and 40 Torr as well as at 1 and 10 atm for the temperature range from 300 to 2100 K.

I. Introduction

A better understanding of the formation of polycyclic aromatic hydrocarbons (PAHs) is of growing scientific interest due to evidence of mutagenic or tumorigenic properties of at least some of them.[1,2] PAHs play an important role in the formation of combustion generated particles such as soot, and their presence in atmospheric aerosols has been shown.[3] The formation of five-membered rings, detected in combustion effluents, is of particular interest due to the potential mutagenic or tumorigenic effect of many of them[4] and their role as intermediates in fullerene formation.[5] The formation of acenaphthylene is of particular interest, since it is one of the most prevalent PAHs. It is suspected of being a major intermediate leading to soot formation, and existing kinetic models give very poor predictions of its concentration in laminar flames.[6,7] A quantitative understanding of the formation of larger and larger PAH molecules, leading ultimately to soot particles, is essential for a better design of efficient and clean practical combustion devices such as engines or incinerators.

A significant contribution of reactions between acetylene, prevalent in the combustion environment of fuel rich hydrocarbon mixtures, and PAH radicals has been suggested on the basis of the concentration profiles of a nearly sooting premixed benzene/oxygen/argon flame measured by means of molecular beam sampling coupled to mass spectrometry.[8] A scheme of subsequent reactions based on the activation of aromatic molecules to radicals by hydrogen abstraction followed by acetylene attack was suggested independently by Bockhorn et al.[9] in a study of premixed hydrocarbon−oxygen flames and by Frenklach et al.[10] investigating shock-tube pyrolysis of acetylene. In a first quantitative study, the latter authors used this hydrogen abstraction/acetylene addition "HACA-mechanism" for the modeling of soot formation and comparison with experimental data. The present work is a detailed study of the HACA acetylene-addition step.

An essential requirement for reliable modeling of PAH growth is the availability of accurate thermodynamic and kinetic parameters. Now that accurate ab initio potential energy surfaces can be computed, the kinetic parameters can be calculated from first principles, using the gas-phase reaction rate theory laid out more than 30 year ago in the classic text by Johnston.[11] The importance of thermodynamic considerations has been pointed out by Stein and Fahr,[12] investigating high-temperature stabilities of hydrocarbons, and Alberty,[13,14] who calculated equilibrium distributions of PAHs in a benzene flame for which experimental data were available.

On the other hand, even relatively small uncertainties on kinetic data may induce substantial deviations on model predictions of PAH concentrations or soot yields due to the accumulation of errors in the large number of subsequent growth steps necessary for the description of the formation of larger compounds. In the past, only a few studies have investigated in detail the elementary steps involved in the HACA mechanism. The rate constant of hydrogen abstraction from benzene, leading to the formation of a reactive phenyl radical, could be deduced experimentally for the reaction $C_6H_6 + H \rightarrow C_6H_5 + H_2$ in a shock-tube study by Kiefer et al.,[15] while the overall rate constant of the $C_6H_6 + OH$ reaction was measured by Madronich and Felder.[16] More recently, Mebel et al.[17] performed a careful ab initio computational study of the $C_6H_5 + H_2$

† Part of the special issue "Harold Johnston Festschrift".
‡ Massachusetts Institute of Technology.
§ New Jersey Institute of Technology.

10.1021/jp002428q CCC: $20.00
Published on Web 12/15/2000

reaction. No kinetic data are available for H-abstraction reactions from PAHs larger than benzene. An ab initio electronic structure study by Cioslowski et al.[18] of the energetics of the homolytic C−H bond cleavage for a series of 10 PAHs between benzene and perylene ($C_{20}H_{12}$) shows no significant impact of the increase of the number of aromatic rings on the C−H bond energies. However, for steric reasons the bond energies are lower in congested "bay" regions of some multiring PAHs. These results seem to indicate only a minor impact of an increasing number of rings on the kinetics of hydrogen abstraction.

Kinetic data on the acetylene-addition step of the HACA scheme have been determined experimentally only for phenyl + acetylene. Fahr and Stein[19] deduced an Arrhenius expression in a temperature range between 1000 and 1330 K in a pyrolytic experiment conducted in a Knudsen cell flow reactor operating at very low pressure (1−10 mTorr) using phenylvinylsulfone as radical source. The shock-tube study of Heckmann et al.[20] confirmed and extended the above rate constant for the temperature range from 1050 to 1450 K.

A deeper insight into this reaction was achieved by Yu et al.[21] They measured absolute constants of phenyl consumption in the temperature range between 297 and 523 K at higher pressure and correlated these results successfully with transition state calculations and the above-mentioned high-temperature data of Fahr and Stein.[19] They suggested the following reaction scheme:

$$C_6H_5 + C_2H_2 \overset{a}{\rightleftarrows} C_6H_5CHCH^{\#} \overset{b}{\rightarrow} C_6H_5C_2H + H$$
$$\overset{c}{\rightarrow} C_6H_5CHCH\ (+M)$$

The vibrationally excited adduct, $C_6H_5CHCH^{\#}$, can decompose to $C_6H_5C_2H$ + H via step b, return to the reactants, C_6H_5 + C_2H_2, or undergo collisional stabilization to produce the thermalized C_6H_5CHCH radical via step c. The effects of temperature and pressure on the total rate and the product branching ratio were assessed by means of the RRKM theory. Yu et al.[21] concluded that the total rate constant, k_t, is independent of the system pressure, whereas the branching ratio is strongly pressure-dependent. Their results show that under the temperature and pressure conditions used by Fahr and Stein,[19] the rate constant of $C_6H_5C_2H$ + H formation, k_b, is equal to k_t, but that at atmospheric pressure combustion conditions a significant formation of stabilized C_6H_5CHCH can be expected.

Cioslowski et al.[22] recently reported a detailed theoretical study on the BLYP/6-311G** level of thermal rearrangements of ethynylarenes to cyclopentafused PAHs, including 1-naphthylacetylene investigated in the present work. They did not attempt to calculate rates, only barrier heights, and did not consider chemical activation/falloff effects. The work of Cioslowski et al.[22] is particularly relevant for high-temperature pyrolysis of PAHs, but the role of the suggested pathways in combustion environments rich in free radicals cannot be excluded. They showed a one-step process involving hydrogen migration immediately followed by ring closure to be energetically favorable and the possibility of hydrogen addition as the initial step of cyclization under certain conditions. In the case of 1-naphthylacetylene, the latter reaction leads to 1-naphthylvinyl, which is the product of the initial addition step of the reaction 1-naphthyl + acetylene studied in the present work. Cioslowski et al.[22] explored the potential energy surface including isomerization reactions to five-membered ring species after 1-naphthylvinyl formation.

Besides the importance of the availability of rate constants determined for a wide temperature range for more realistic numerical modeling, the possibility of more significant C_6H_5CHCH formation under certain combustion conditions could lead to a reconsideration of the role of acetylene adducts in the growth process of PAHs, initially suggested by Bittner and Howard[8] and described as a minor route by Frenklach et al.[10]

The identification of PAHs up to ovalene ($C_{32}H_{14}$) by means of chromatographic techniques in low pressure[23] and atmospheric pressure[24] combustion also gives rise to the question of the variation in total rate constants and branching ratios of acetylene attack to PAH radicals at different temperatures and pressures as a function of molecule size. In a first attempt, Wang and Frenklach[25] determined the rate constants for benzene and PAH growth up to the formation of pyrene ($C_{16}H_{10}$) using semiempirical quantum-mechanical calculations and transition state theory and assessed pressure dependence by means of the RRKM approach and included the resulting rate constants in a detailed modeling study of laminar premixed acetylene and ethylene flames.[26] Recent modeling studies reveal an increasing understanding of the kinetics of PAH formation; nevertheless, significant disagreements between model predictions and experimental data, as shown recently for a premixed benzene flame,[6] remain unexplained. Therefore, the determination of reliable kinetic data for reaction steps contributing to PAH growth as well as the comparison of the updated kinetic models with experimental data is needed.

II. Computational Approach

In the present work, a systematic theoretical study of acetylene addition to phenyl and 1-naphthyl, radicals of the first two species of the homologous series of polycyclic aromatic hydrocarbons, is presented. The potential energy surfaces are carefully explored and transition states determined using density functional theory calculations. The density functional calculations are checked using Hartree−Fock-based quantum chemistry calculations including electron correlation.

Chemical activation, i.e., the contribution of energy present in internal degrees of freedom for further reactions of the initial adduct prior to thermalization, is taken into account using well-established methods,[27−30] as implemented in a substantially improved multiwell version of CHEMDIS.[31] In the initial version[30] of CHEMDIS, the effects of collisional energy transfer are approximated using the modified strong collision approach developed by Troe and co-workers.[32] For increased accuracy, in the new CHEMDIS[31] the effective collision parameter β is approximated using the higher order formula suggested by Gilbert et al.[33] The new CHEMDIS software is capable of treating complex situations with a large number of isomers with a set of reactions connecting the wells to each other in any topology, a feature which is critical for accurately modeling the complex chemically activated isomerizations which follow the addition of 1-naphthyl to acetylene. The chemical activation analysis allows the determination of apparent rate constants $k(T,P)$ for the different reaction channels relative to the reactants.

CHEMDIS and the related THERFIT software developed by Dean, Bozzelli, and co-workers take as input the high-pressure-limit rates $k_\infty(T)$ and thermochemical information on all of the species and elementary-step reactions involved in a chemically activated reaction network.[30,31] For the pressure-dependence calculation, the corresponding microcanonical quantities are needed and are computed by CHEMDIS from the Boltzmann-averaged quantities. The required densities of states, $\rho(E)$, are computed from the heat capacities fitted to the three-frequency form proposed by Bozzelli and co-workers, using their THER-

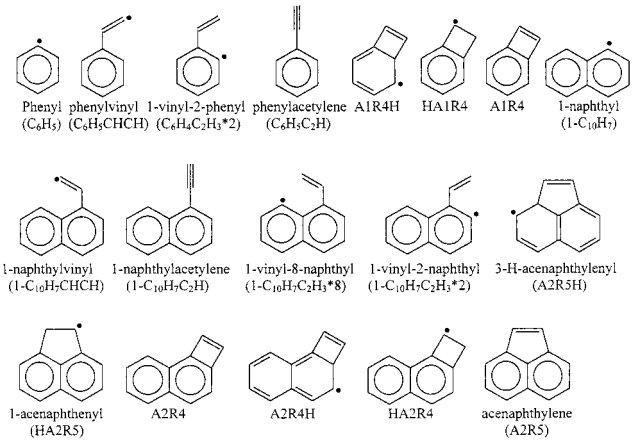

Figure 1. Molecular structures of species considered in the present work.

FIT software.[34] The microcanonical rates $k(E)$ required for the chemical activation analysis are computed from the high-pressure-limit $k_\infty(T)$ values by the QRRK method developed by Dean.[27] Note that for Arrhenius forms $k_\infty(T) = Ae^{-E_a/RT}$ the QRRK method obtains exactly the same $k(E)$ the inverse-Laplace transform (ILT) technique pioneered by Forst.[35] The bath gas is assumed to be argon in the present work, but the use of another bath gas such as nitrogen or helium showed only an insignificant impact on the predicted rate constants. Therefore, we expect that the rate constants obtained in the present work will be valid for a wide range of combustion mixtures.

Density functional theory calculations on all involved species were carried out with the DGAUSS program[36] within the UniChem[37] package using the BLYP functional[38,39] in conjunction with the DZVP basis set.[40] Vibrational analysis performed on the optimized geometries allowed the determination of entropies and heat capacities. Heats of formation were taken from the NIST database,[41] if available. For species for which no value was recommended, as was the case for most radical species, the DFT energies added to the zero-point vibrational energy and the temperature-dependent enthalpy correction were used for the determination of reaction enthalpies of isodesmic reactions, i.e., reactions which maintain the overall number and types of bonds. With the heats of formation of the other compounds involved in the reaction being known, the value of the studied species can be deduced. The careful choice of the used isodesmic reaction allowed evaluation of heats of formation to accuracies approaching the sum of the uncertainties of the other—often experimental—values involved in the isodesmic reactions. The molecular structures of all species considered in the present work are shown in Figure 1, and the thermodynamic properties are summarized in Table 1. The thermodynamic properties are converted into NASA polynomial format by means of the subroutine THERMFIT of the THERM software,[42] which is convenient for thermodynamic, kinetic, and equilibrium calculations. The precision of the thermodynamic data depends on the uncertainty resulting from the density functional theory computation, errors induced by simplifications of the vibrational analysis for the determination of heat capacities and entropies, and in the case of heats of formation deduced by means of isodesmic reactions on the margin of uncertainties of the involved literature data. Comparison with literature data, e.g. for styrene as discussed below, indicates an uncertainty within 5 J mol^{-1} K^{-1} for entropies and heat capacities. On the basis of an uncertainty of ± 8 kJ mol^{-1} for the literature recommendation of the heat of formation of phenyl,[41] a potential error of about ± 10 kJ mol^{-1} must be assumed.

To evaluate the rate constants of the elementary reactions, we performed the density functional computations on the reactants, reaction intermediates, products, and the corresponding transition states using GAUSSIAN98.[43] Each transition state was connected to the corresponding minima by visualization of its normal mode with a negative eigenvalue. Vibrational frequencies of all structures were calculated using the BLYP functional with Dunning's correlation consistent cc-pVDZ basis set.[44] Low-frequency vibrations (those below 300 cm^{-1}), high-frequency vibrations, and zero-point vibration energies were then scaled by factors of 1.0667, 0.9986, and 1.0167, respectively.[45]

Geometries of all isomers and transition states were further optimized using the Becke three-parameter hybrid functional combined with the Lee, Yang, and Parr correlation (B3LYP) density functional theory method[46] with the cc-pVDZ basis set. The reaction barriers were calculated as the difference between the B3LYP/cc-pVDZ + ZPE(BLYP/cc-pVDZ) energies of the corresponding stable and transition state structures. For the structures involved in H-loss reactions, vibrational frequencies were also calculated at the B3LYP/cc-pVDZ level of theory. Low frequencies, high frequencies, and zero-point vibrational energies of these species were scaled by 1.0013, 0.9614, and 0.9806, respectively.[45] The B3LYP transition state geometries are provided in the Supporting Information.

Subsequently, to test the accuracy of the density functional calculations with a different quantum chemistry method, we carried out single-point spin-restricted Mœller−Plesset[47] calculations (ROMP2/cc-pVDZ//B3LYP/cc-pVDZ) for comparisons. It was found that the relative energies of all structures with respect to the energy of 1-naphthylvinyl (see Figure 1) calculated by three different methods agree within 12 kJ/mol. The exceptions are the ROMP2 energies of the 3-H-acenaphthylenyl (A2R5H) and of the transition state linking the 3-H-acenaphthylenyl with the 1-acenaphthenyl (HA2R5) (see Figure 1). For these cases, the differences between relative energies calculated at the B3LYP and ROMP2 levels of theory are ~16 and 24 kJ/mol, respectively. Our previous experience suggests that for this particular case the error primarily lies in the ROMP2 calculation.

Our conclusion is that these density functional calculations are all accurate to better than 20 kJ/mol. The isodesmic calculations on the stable structures are expected to be much more accurate; we estimate an uncertainty of 10 kJ/mol (much of which comes from uncertainties in the experimental thermochemical data on the species used to derive the isodesmic values.)

Transition states were identified and corresponding high-pressure-limit rate constants were calculated from the conventional (fixed geometry) transition state theory:[11]

$$k = \frac{k_B T}{h} \frac{Q_{TS}}{Q_R} \exp(-E/k_B T)$$

where Q_{TS} and Q_R are the partition functions of the transition state and reactants, respectively, and E is the reaction barrier, making the ordinary approximations of assuming that the degrees of freedom are separable, and then evaluating their contribution to the partition functions using rigid-rotor and harmonic-oscillator models. As input to the TST program we gave the geometries and vibrational frequencies of the reactants and of the transition state, moments of inertia of the internal rotors of the reactants and transition state, the reaction barrier corrected for the zero-point energies, and the symmetry numbers of the reactants and transition state. The resulting high-pressure-

TABLE 1: Thermodynamic Data of Species Considered in the Present Work (units: ΔH_f^0, kJ mol^{-1}; S_f^0, C_p, J mol^{-1} K^{-1})

species	ΔH_f^0	S_f^0	$C_{p,300K}$	$C_{p,400K}$	$C_{p,500K}$	$C_{p,600K}$	$C_{p,800K}$	$C_{p,1000K}$	$C_{p,1500K}$	ref
H	218.0[a]	114.7	20.79	20.79	20.79	20.79	20.79	20.79	20.79	41
C_2H_2	226.7[a]	200.9	44.2		54.83		63.77	68.25	76.65	41
C_6H_5	339[a]	284.5	83.3	110.9	133.4	151.7	178.6	196.6	222.7	41, pw[c]
C_6H_5CHCH	404[b]	347.3	127.7	163.5	192.5	215.9	250.2	273.6	309.5	pw
$C_6H_4C_2H_3$*2	399[b]	345.9	122.7	159.5	189.3	213.4	248.7	272.8	309.2	pw
$C_6H_5C_2H$	307[a]	341.6	124.7	156.8	183.0	204.4	235.8	257.2	288.9	pw
A1R4H	470[b]	326.6	117.1	156.1	187.6	213.0	249.9	274.3	309.7	pw
HA1R4	377[b]	329.1	117.6	155.5	186.5	211.7	248.7	273.5	309.2	pw
A1R4	429[b]	324.8	112.9	148.4	177.2	200.4	234.1	256.4	289.0	pw
1-$C_{10}H_7$	406[b]	347.9	135.1	179.6	215.7	244.9	287.3	315.3	355.0	53
1-$C_{10}H_7CHCH$	469[b]	396.6	174.9	229.1	272.7	307.8	358.5	392.4	442.2	pw
1-$C_{10}H_7C_2H$	371[b]	395.9	173.0	222.8	263.3	296.0	343.8	375.4	420.8	pw
1-$C_{10}H_7CHCH$*8	468[b]	399.4	173.5	227.6	271.2	306.3	357.3	391.4	441.7	pw
1-$C_{10}H_7CHCH$*2	472[b]	385.8	164.9	219.0	262.7	298.0	349.3	383.3	432.7	pw
A2R5H	383[b]	372.1	163.5	220.0	265.9	302.9	356.6	391.9	441.6	pw
HA2R5	285[b]	373.7	164.8	220.6	265.9	302.6	356.0	391.2	441.3	pw
A2R4	477[b]	380.3	163.7	216.1	258.6	292.9	342.6	375.2	421.3	pw
A2R4H	492[b]	384.6	167.6	223.3	268.4	304.8	357.8	392.5	441.9	pw
HA2R4	409[b]	383.8	167.6	222.6	267.4	303.7	356.7	391.8	444.4	pw
A2R5	258[a]	349.7	157.2	210.9	254.4	289.5	340.3	373.6	420.6	41, pw

[a] Heat of formation taken from the NIST database.[41] [b] Heat of formation calculated by means of isodesmic reaction. [c] pw: present work.

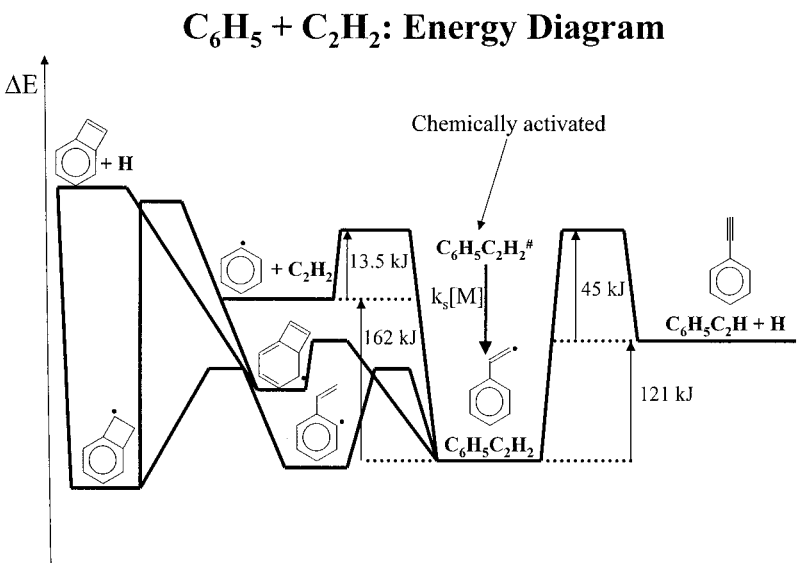

Figure 2. Potential surface of the reaction $C_6H_5 + C_2H_2$.

limit rate constants $k_\infty(T)$ are fitted to the expression $k_\infty(T) = AT^n e^{-Ea/RT}$ over a temperature range from 300 to 2100 K. The effect of tunneling was tested for the reactions involving hydrogen transfer and loss using the Wigner perturbation theory expression, but was shown to be insignificant even at room temperature.

Beginning the investigation with phenyl + C_2H_2 allowed the comparison of the chosen approach with available data[19−21] before moving on to the more poorly understood reaction of interest, 1-naphthyl + C_2H_2. Thus, the apparent rate constants $k(T,P)$ of the formation of phenylacetylene via the reaction

$$C_6H_5 + C_2H_2 \rightarrow C_6H_5C_2H + H \quad (1)$$

and of the adduct C_6H_5CHCH through

$$C_6H_5 + C_2H_2 \rightarrow C_6H_5CHCH \quad (2)$$

were determined first.

On the basis of the similarity of the reactants, the reaction of 1-naphthyl with acetylene is likely to follow a similar sequence to the reaction of phenyl with acetylene. Nevertheless, the possibility of ring closure adds an essential feature, and the relative yield of acenaphthylene is of significant interest. The apparent rate constants of the following three reactions are particularly important for combustion models:

$$1\text{-}C_{10}H_7 + C_2H_2 \rightarrow 1\text{-}C_{10}H_7C_2H + H \quad (3)$$

$$1\text{-}C_{10}H_7 + C_2H_2 \rightarrow 1\text{-}C_{10}H_7CHCH \quad (4)$$

$$1\text{-}C_{10}H_7 + C_2H_2 \rightarrow \text{acenaphthylene} + H \quad (5)$$

To show the sensitivity of the $k(T,P)$ calculations to the uncertainties in the quantum chemistry and TST calculations, error bars are included in the figures. They reflect the effects of changing the activation energies by ±4 kJ/mol and the frequencies of both the reactants and transition states by ±15 cm^{-1}. The latter value has been reported as the typical uncertainty of B3LYP vibrational frequencies.[45]

III. Results and Discussion

A. Phenyl + C_2H_2. Our exploration of the potential energy surface of acetylene addition to phenyl radicals confirmed basically the picture of Yu et al.,[21] presented above, but led to the identification of additional pathways involving four-membered ring species and intramolecular hydrogen abstraction. A schematic energy diagram is shown in Figure 2, and the identified transition states are given in the Supporting Informa-

tion. A transition state allowing for internal hydrogen abstraction from the aromatic ring of phenylvinyl to 1-vinyl-2-phenyl, shown in reaction 6, has been identified:

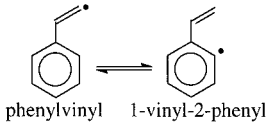

(6)

Frenklach and co-workers[48] have noted the importance of reactions similar to reaction 6.

Pathways leading to cyclization of both species to four-membered-ring-containing radicals have been identified as well as isomerization between the latter species.

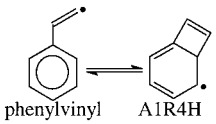

(7)

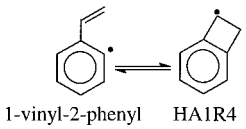

(8)

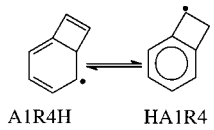

(9)

No transition states allowing for the direct isomerization of phenylvinyl to HA1R4 nor of 1-vinyl-2-phenyl to A1R4H could be found. Forward and reverse rate constants of reactions 6−9 were computed by means of transition state theory. Both A1R4H and HA1R4 can lose hydrogen in a subsequent step and form A1R4, reactions (10) and (11). Corresponding rate constants were deduced by means of transition state theory. More than a dozen additional minima have been identified on the potential energy surface. These minima and the corresponding transition states are given in the Supporting Information. Virtually all of these minima and transition states are thermodynamically prohibitive. Inclusion in the QRRK treatment of the relatively low-energy pathway leading to formation of 1-vinyl-3-phenyl and 1-vinyl-4-phenyl after hydrogen migration beginning with 1-vinyl-2-phenyl does not significantly affect any of the major reaction channels.

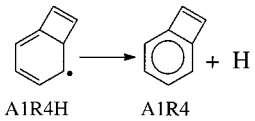

(10)

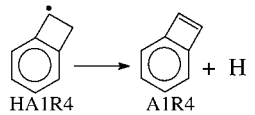

(11)

The high-pressure-limit rate constant of the entrance channel (12), i.e., the formation of the adduct phenylvinyl (C_6H_5CHCH) from the reactants phenyl and acetylene (reaction "a" in Yu et al.'s scheme) was also computed.

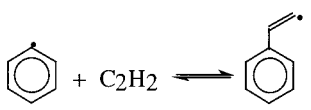

(12)

A potential uncertainty on the preexponential factor stems from the treatment of the phenyl−CHCH bond torsion as internal rotation or harmonic vibration. To assess the appropriate approach, the energy barrier for rotation around the aryl−CHCH axis was determined for 1-naphthylvinyl starting with the BLYP/DZVP-optimized geometry of the stabilized species. An energy barrier of 9.0 kJ was obtained and the comparison of the rate constants deduced with both the harmonic oscillator and internal rotor approaches showed nearly identical values at 2100 K, the upper end of the temperature range covered in the present work. At room temperature the vibrational treatment yielded a 50% smaller value. On the basis of these findings aryl−CHCH bonds are exclusively treated as harmonic oscillators in the present work. The accuracy of this approach was confirmed indirectly by means of the excellent agreement (± 4 J mol^{-1} K^{-1}) between experiment and the predictions (using the harmonic oscillator treatment) of the entropy and heat capacities of styrene. A high-pressure limit of the reaction 12 of $k_{12} = (3.14 \times 10^7)T^{1.767}\exp(-13540\ J/RT)$ cm^3 mol^{-1} s^{-1} for the temperature range from 300 to 2100 K was computed on the basis of density functional and transition state theory and used as input for the chemical-activation analysis. The high-pressure limit rate constant is shown in Figure 3a−d and is between about 2.5 (at room temperature) and 10 times (at 2100 K) higher than the one suggested by Yu et al.;[21] the latter rate constant was obtained by adjusting the transition state parameters to match an experimental rate constant measured at room temperature and 20 Torr by means of the cavity-ring-down technique.[21]

The high-pressure-limit rate constant for reaction 13, hydrogen loss from phenylvinyl to form phenylacetylene (reaction "b" in Yu et al.'s scheme), has also been computed using transition state theory. The barrier height of 166 kJ mol^{-1} is in excellent agreement with the value obtained by Yu et al.[21] using BAC-MP4 computations.

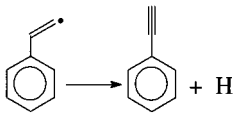

(13)

As pointed out by Yu et al.,[21] quantitative correlation of the different data sets measured at different temperatures and pressures requires the treatment of the phenyl + acetylene reaction as chemically activated. Similar to the approach of Yu et al.,[21] but adding intramolecular hydrogen transfer and the formation of four-membered ring species, the reaction C_6H_5 + C_2H_2 is described as followed:

$$C_6H_5 + C_2H_2 \rightarrow C_6H_5CHCH^{\#}: \text{ formation of chemically activated molecule} \quad (14)$$

The input parameters for the chemical-activation computations

$$C_6H_5CHCH^{\#} \rightarrow C_6H_5 + C_2H_2\text{: dissociation} \quad (-14)$$

$$C_6H_5CHCH^{\#} + M \rightarrow C_6H_5CHCH + M\text{: stabilization} \quad (15)$$

$$C_6H_5CHCH^{\#} \rightarrow C_6H_5C_2H + H\text{: decomposition} \quad (16)$$

$$C_6H_5CHCH^{\#} \leftrightarrows C_6H_4C_2H_3{*}2\text{: isomerization} \quad (17)$$

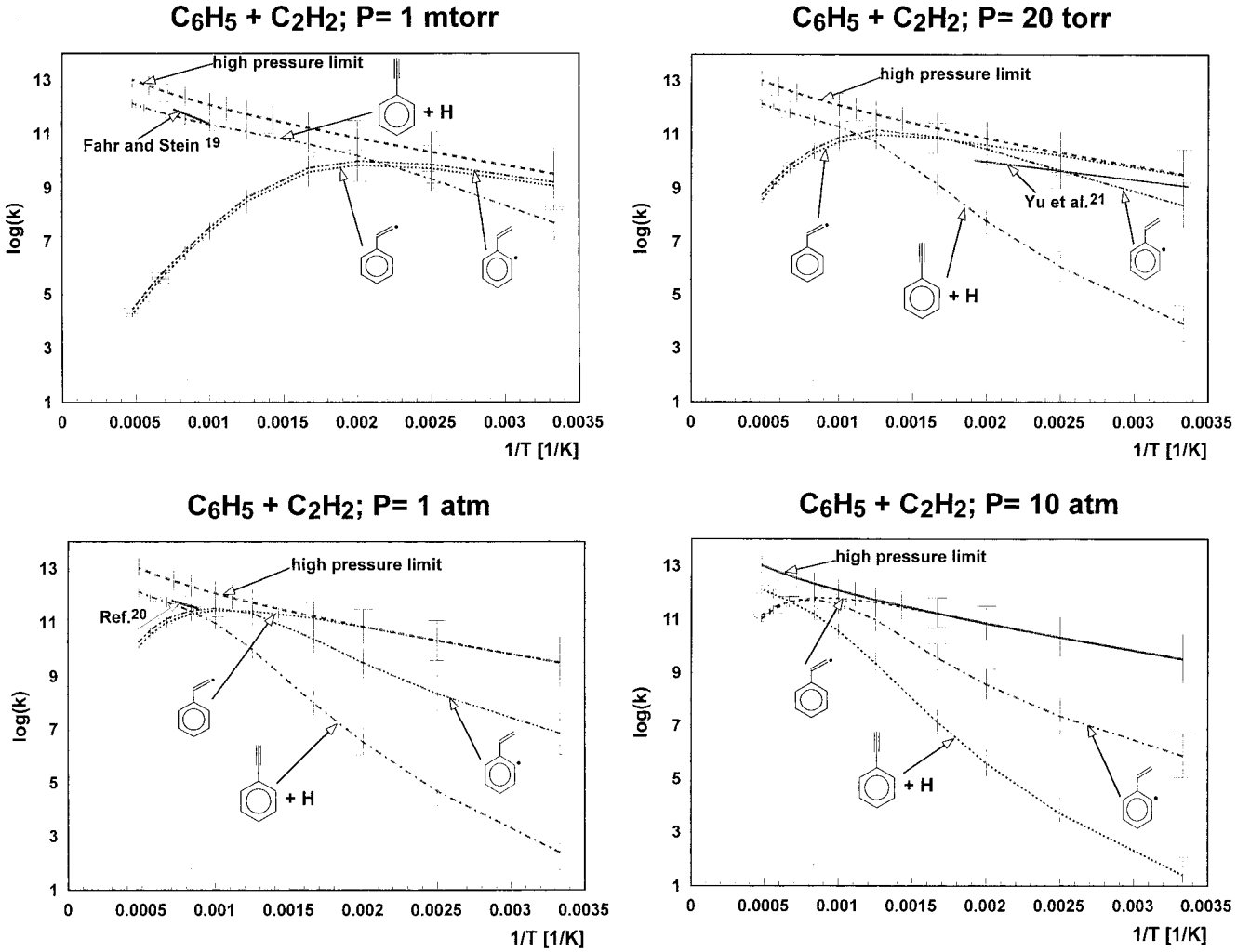

Figure 3. Computed rates for the reaction $C_6H_5 + C_2H_2$ to form various products: ---, high-pressure limit; —, experimental data (Fahr and Stein[19], Yu et al.[21], Heckmann et al.[20]); ▪▪▪, apparent rate constant of $C_6H_5 + C_2H_2 \rightarrow C_6H_5CHCH$; •—•—, apparent rate constant of $C_6H_5 + C_2H_2 \rightarrow C_6H_5C_2H + H$; ▪▪—▪▪—, apparent rate constant of $C_6H_5 + C2H2 \rightarrow C_6H_4C_2H_3 \times 2$. (a) $P = 1$ mTorr, (b) $P = 20$ Torr, (c) $P = 1$ atm, (d) $P = 10$ atm.

$$C_6H_5CHCH^{\#} \leftrightarrows \text{A1R4H: isomerization} \quad (18)$$

$$C_6H_4C_2H_3 \times 2 \leftrightarrows \text{HA1R4: isomerization} \quad (19)$$

$$\text{A1R4H} \leftrightarrows \text{HA1R4: isomerization} \quad (20)$$

$$\text{A1R4H} \rightarrow \text{A1R4} + \text{H: decomposition} \quad (21)$$

$$\text{HA1R4} \rightarrow \text{A1R4} + \text{H: decomposition} \quad (22)$$

are summarized in Table 2. All computations in the present work were conducted in the temperature range between 300 and 2100 K and at pressures of 1 mTorr, 20 and 40 Torr, and 1 and 10 atm, covering the conditions usually relevant for combustion processes as well as the low-pressure experiments of Fahr and Stein.[19] The pressure dependence of the branching ratio between the stabilization reaction 15 and formation of phenylacetylene via the decomposition reaction 16 is particularly interesting. The rate constant of the dissociation (−14) has been determined by means of the equilibrium constant of $C_6H_5 + C_2H_2 \rightarrow C_6H_5CHCH$ with all thermodynamic data being calculated using ab initio techniques as detailed above and summarized in Table 1. σ and ϵ/k_b are the Lennard-Jones parameters, i.e., the collision diameter and the well depth given for the initial adduct as well as for the bath gas, and $<\Delta E>$ represents the average energy transferred per collision between the adduct and the bath gas.

The resulting apparent rate constants for the formation of the stabilized adduct, C_6H_5CHCH, and of phenylacetylene, $C_6H_5C_2H$, are shown in Figure 3a−d for 1 mTorr, 20 Torr, and 1 and 10 atm, with experimental data available for the first three

TABLE 2: Inputs for Chemical Activation Analysis of $C_6H_5 + C_2H_2$

parameter	used in present work
k_1 ($cm^3\ mol^{-1}\ s^{-1}$)	$(3.14 \times 10^7)T^{1.767} \exp(-13.54\ kJ/RT)$
→ C_6H_5CHCH: σ (Å)	5.646[50]
→ C_6H_5CHCH: ϵ/k_b (K)	450.0[50]
	Well 1: C_6H_5CHCH
→ $C_6H_5 + C_2H_2$	$(2.86 \times 10^{10})T^{1.486} \exp(-174\ kJ/RT)$
→ $C_6H_5C_2H + H$	$(1.37 \times 10^9)T^{1.575} \exp(-166\ kJ/RT)$
→ $C_6H_4C_2H_3 \times 2$	$(5.03 \times 10^9)T^{0.887} \exp(-96\ kJ/RT)$
→ A1R4H	$(1.50 \times 10^{10})T^{0.648} \exp(-130\ kJ/RT)$
	Well 2: $C_6H_4C_2H_3$*2
→ C_6H_5CHCH	$(1.05 \times 10^9)T^{0.995} \exp(-93\ kJ/RT)$
→ HA1R4	$(4.85 \times 10^9)T^{0.727} \exp(-119\ kJ/RT)$
	Well 3: A1R4H
→ C_6H_5CHCH	$(4.43 \times 10^{11})T^{0.471} \exp(-53\ kJ/RT)$
→ HA1R4	$(1.37 \times 10^{11})T^{0.639} \exp(-166\ kJ/RT)$
→ A1R4 + H	$(5.12 \times 10^9)T^{1.325} \exp(-202\ kJ/RT)$
	Well 4: HA1R4
→ $C_6H_4C_2H_3$*2	$(2.33 \times 10^{11})T^{0.643} \exp(-140\ kJ/RT)$
→ A1R4H	$(4.64 \times 10^{10})T^{0.840} \exp(-261\ kJ/RT)$
→ A1R4 + H	$(3.14 \times 10^7)T^{2.386} \exp(-295\ kJ/RT)$
argon: σ (Å), ϵ/k (K), $\langle \Delta E \rangle$ ($J\ mol^{-1}$)	3.33, 136.5, 2636[30]

TABLE 3: Rate Constants for $C_6H_5 + C_2H_2 \rightarrow C_6H_5CHCH$, $C_6H_5 + C_2H_2 \rightarrow C_6H_4C_2H_3$*2, and $C_6H_5 + C_2H_2 \rightarrow C_6H_5C_2H + H$ between 300 and 2100 K at 20 and 40 Torr, 1 and 10 atm

reaction	$k_{20\text{Torr}}$ ($cm^3\ mol^{-1}\ s^{-1}$)	$k_{40\text{Torr}}$ ($cm^3\ mol^{-1}\ s^{-1}$)	$k_{1\text{atm}}$ ($cm^3\ mol^{-1}\ s^{-1}$)	$k_{10\text{atm}}$ ($cm^3\ mol^{-1}\ s^{-1}$)
$\rightarrow C_6H_5CHCH$	$(8.6 \times 10^{44})T^{-10.50} \exp(-55\ kJ/RT)$	$(1.4 \times 10^{43})T^{-9.87} \exp(-54\ kJ/RT)$	$(6.7 \times 10^{34})T^{-7.04} \exp(-46\ kJ/RT)$	$(2.3 \times 10^{27})T^{-4.56} \exp(-38\ kJ/RT)$
$\rightarrow C_6H_4C_2H_3$*2	$(7.9 \times 10^{51})T^{-12.41} \exp(-74\ kJ/RT)$	$(6.1 \times 10^{50})T^{-11.97} \exp(-76\ kJ/RT)$	$(1.1 \times 10^{41})T^{-8.61} \exp(-76\ kJ/RT)$	$(5.2 \times 10^{27})T^{-4.38} \exp(-66\ kJ/RT)$
$\rightarrow C_6H_5C_2H + H$	$(8.3 \times 10^{22})T^{-2.68} \exp(-73\ kJ/RT)$	$(8.1 \times 10^{21})T^{-2.36} \exp(-73\ kJ/RT)$	$(1.8 \times 10^{16})T^{-0.62} \exp(-73\ kJ/RT)$	$(1.5 \times 10^{9})T^{1.51} \exp(-69\ kJ/RT)$

pressures. The indicated uncertainties are based on the above-mentioned variations of the high-pressure rate constants of the entrance channel (14) and of the corresponding reverse reaction (−14) as well as of the hydrogen loss reaction 16. The largest deviation has been plotted. The comparison with the low-pressure measurements of Fahr and Stein[19] between 1000 and 1330 K (Figure 3a) but also with the shock tube study of Heckmann et al.[20] (Figure 3c) at slightly higher temperatures with the apparent rate constant of phenylacetylene formation is encouraging. The computed data are 2.5 times—or less—smaller than the literature data, an excellent agreement considering experimental and computational uncertainties, in particular competing reactions such as biphenyl formation, to be taken into account for the deduction of experimental rate constants. A larger deviation was observed relative to the 20 Torr data measured by Yu et al.[21] between 297 and 523 K using the cavity-ring-down technique. The experimental value at room temperature[21,49] is 2.5 times lower than the computed one, and the deviation is increasing to a factor of about 4 at the upper limit of the measured temperature range. However, the experimental data still remain inside the uncertainty of the computed rate constant for phenylvinyl formation. The satisfactory agreement at low and intermediate temperatures and the consistency with two independent studies above 1000 K and different pressures give us a high level of confidence in the present rate constants. With increasing pressure the high-pressure limit is reached by the addition reaction 2 for higher and higher temperatures. Nevertheless, even at 10 atm the system does not reach the high-pressure-limit at the upper end of the investigated temperature range, even though the density of states of this 15-atom polyatomic adduct is enormous. Apparent rate constants for the formation of the stabilized adduct (phenylvinyl radical, C_6H_5CHCH), and of phenylacetylene, $C_6H_5C_2H$, are summarized in Table 3 for 20 and 40 Torr and 1 and 10 atm covering the temperature range from 300 to 2100 K. The relative importance of the formation of the stabilized adduct, C_6H_5CHCH, and of the product channel $C_6H_5C_2H + H$ changes as expected with temperature and pressure. Figure 3a−d shows that formation of phenylacetylene is the dominant pathway at high temperatures and low pressures, and the rate constant is continuously increasing with temperature and is in good agreement with the low-pressure measurement of Fahr and Stein[19] and the shock tube data of Heckmann et al.[20] C_6H_5CHCH formation is dominant at low temperatures, and its rate constant exhibits a maximum which is shifting to higher and higher temperatures with increasing pressure. Therefore, C_6H_5CHCH should be considered as a potential intermediate for further growth reactions in high-pressure combustion, leading, for example, to naphthalene, as initially suggested by Bittner and Howard.[8] Our calculations show also the possibility of significant formation of 1-vinyl-2-phenyl which has been suggested by Frenklach et al.[48] as an intermediate for naphthalene formation in the case of 1,3-butadiene pyrolysis. The corresponding apparent rate constants are shown in Figure 3a−d and given in Table 3. The evolution with temperature and pressure of the rate constants is similar to that of the formation of phenylvinyl; i.e., the rate constant exhibits an increasing maximum shifting to higher temperatures with increasing pressure. Contrary to phenylvinyl with a rate constant approaching the high-pressure limit at lower temperatures, increasing pressure induces a significant decrease of the apparent rate constant describing 1-vinyl-2-phenyl formation at low and intermediate temperatures.

With the formation of the four-membered ring species A1R4H, HA1R4, and A1R4 being included in the chemical activation analysis, apparent rate constants of their formation have been determined. The rate constant of the apparent reaction

$$C_6H_5 + C_2H_2 \rightarrow A1R4 + H \qquad (23)$$

exhibits a strong temperature dependence which increases with the pressure but reaches only a value of about 2.2×10^9 $cm^3\ mol^{-1}\ s^{-1}$ at 2100 K and 10 atm. The thermodynamic equilibrium of this reaction, which is entirely shifted to the reactants at room-temperature, moves to the right side with increasing temperature but is still unfavored for the formation of A1R4 at the upper limit of the temperature range studied in the present work. The formation of A1R4H via

$$C_6H_5 + C_2H_2 \rightarrow A1R4H \qquad (24)$$

is thermodynamically favored at low temperatures close to room temperature, while the equilibrium is progressively shifting to the reactants with increasing temperature. The apparent rate is strongly pressure-dependent and exhibits a maximum which is increasing and shifting to higher temperatures with increasing pressure. Nevertheless, no rate constant higher than about 10^9 $cm^3\ mol^{-1}\ s^{-1}$ was determined, the latter obtained at 10 atm and between 1000 and 1500 K, already a thermodynamically unfavorable temperature range.

Therefore, the formation of A1R4 and A1R4H was shown to be significantly slower than the competing pathways and can be neglected in usual combustion or pyrolytic environments. As shown in Figure 2, HA1R4 is thermodynamically the most stable of all C_6H_5CHCH isomers and the apparent rate constant of its formation via reaction 25 ($C_6H_5 + C_2H_2 \rightarrow$ HA1R4) can be as large as 10^{11} $cm^3\ mol^{-1}\ s^{-1}$, significantly higher than for the formation of A1R4H and A1R4 + H. Temperature and pressure dependence are similar to the formation of C_6H_5CHCH and $C_6H_4C_2H_3$*2. Nevertheless, a significant contribution of HA1R4 to reaction networks relevant to combustion chemistry is unlikely, due to the absence of a viable exit channel, the formation of A1R4 being unfavorable.

As shown in Figure 3a−d, no reaction channel reaches the high-pressure limit above about 1000 K for the pressures investigated in the present study, i.e., up to 10 atm. In existing chemical kinetic models of combustion, the pressure dependence of most reactions involving such large adducts is ignored, and the rates are assumed to be close to the high-pressure limit. The present work suggests that chemical-activation effects and pressure-dependence are important in a much broader range of reactions than has been assumed.

The comparison of the calculations on the phenyl + C_2H_2 reaction with the experimental data suggests that our computational approach is at least reasonable, suggesting that the calculations on the larger 1-naphthyl + C_2H_2 system may also be reliable.

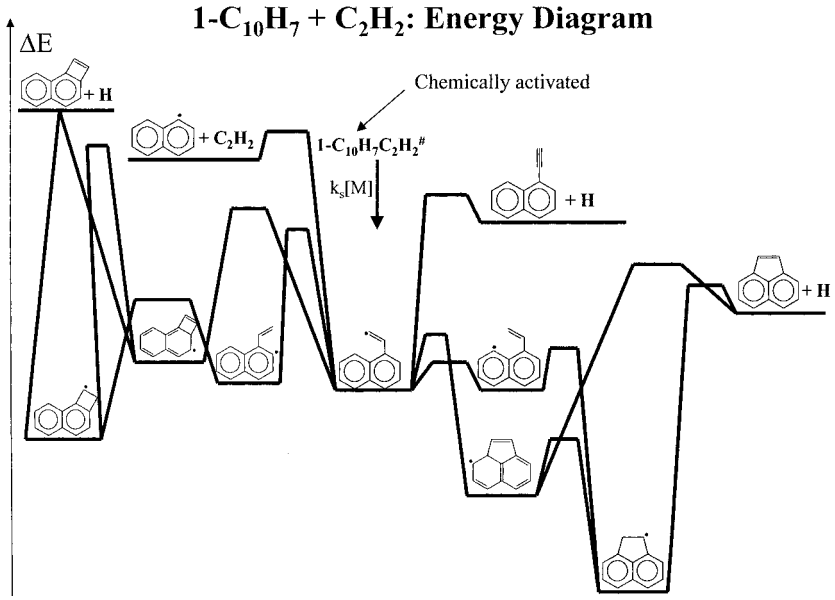

Figure 4. Schematic potential energy surface of the reaction 1-$C_{10}H_7$ + C_2H_2.

B. 1-Naphthyl + C_2H_2. The potential surface of the reaction between 1-naphthyl radicals and acetylene has been explored and is shown in Figure 4. An essential additional feature is the possible formation of acenaphthylene, the first species of an important series of PAH compounds containing five-membered rings. Pertinent to the present work, electronic structure calculations in order to elucidate the reaction mechanism of the thermal rearrangement of ethynylarenes to cyclopentafused PAHs, including formation of acenaphthylene from 1-naphthylacetylene, have been reported recently.[22] Similar to phenyl + acetylene, the first step of the reaction sequence is the formation of a chemically activated molecule:

$$1\text{-}C_{10}H_7 + C_2H_2 \rightarrow 1\text{-}C_{10}H_7CHCH^{\#} \qquad (26)$$

The corresponding rate constant at the high-pressure limit was obtained in the present work by means of transition state theory and the expression $k_{26} = (1.87 \times 10^7)T^{1.787}\exp(-13\,650\ \mathrm{J}/RT)$ $\mathrm{cm^3\ mol^{-1}\ s^{-1}}$ was used as input for the chemical-activation analysis.

The chemically activated molecule can reform the reactants (−26), be stabilized via reaction with a third body (27), decompose, i.e., lose a hydrogen (28), or undergo different isomerization reactions, leading ultimately to acenaphthylene (A2R5).

$$1\text{-}C_{10}H_7CHCH^{\#} \rightarrow 1\text{-}C_{10}H_7 + C_2H_2 \qquad (-26)$$

$$1\text{-}C_{10}H_7CHCH^{\#} + M \rightarrow 1\text{-}C_{10}H_7CHCH + M \qquad (27)$$

$$1\text{-}C_{10}H_7CHCH^{\#} \rightarrow 1\text{-}C_{10}H_7C_2H + H \qquad (28)$$

The rate constant of the dissociation (−26) was determined by means of transition state theory. Its independent calculation using the equilibrium constant of the reaction 1-$C_{10}H_7$ + C_2H_2 ⇆ 1-$C_{10}H_7$CHCH using the thermodynamic data summarized in Table 1 gave very similar results and therefore confirms the consistency of the data used in the present work. Exact Lennard-Jones parameters for the initial adduct are not available, so those suggested by Pope[50] for acenaphthylene were used. The isomerization reactions are relatively complex and deserve therefore more detailed discussion. The exploration of the potential surface has revealed several reactions of the initial adduct 1-naphthylvinyl (1-$C_{10}H_7$CHCH).

As initially suggested by Wang and Frenklach,[25] an internal ring-closure can lead to 3-H-acenaphthylenyl (A2R5H) and form acenaphthylene by subsequent hydrogen loss:

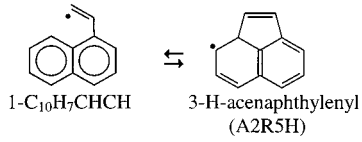

(29)

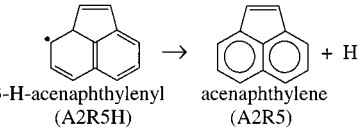

(30)

The transition state of reactions 29 and 30 have been determined and the rate constants of the forward and the reverse reactions were deduced by means of unimolecular transition state theory.

The vinyl group of 1-$C_{10}H_7$CHCH can also abstract hydrogen atoms from adjacent carbon atoms in intramolecular reactions. The corresponding transition states were found and rate constants for forward and reverse reactions determined.

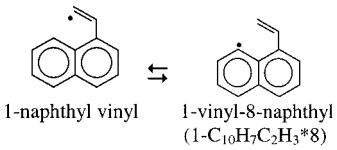

(31)

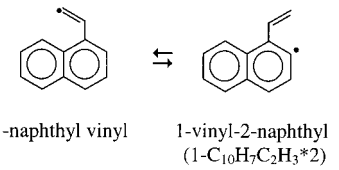

(32)

The possibility of reactions 31 and 32 is obviously related to the hindered internal rotation of the vinyl group, which has an energy barrier of about 9 kJ, as discussed above. Another

identified transition state allows the reaction of 1-vinyl-8-naphthyl to 1-acenaphthenyl (HA2R5), as shown in reaction 33 and for which the corresponding kinetic data could be deduced.

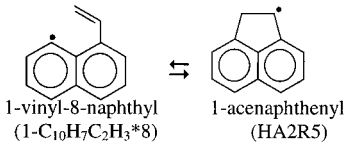

(33)

The potential role of 1-acenaphthenyl in the formation of five-membered rings has already been discussed by Cioslowski et al.,[18] but they did not consider 1-vinyl-8-naphthyl as an intermediate and attributed the transition state of reaction 33 to a direct isomerization step from 1-naphthylvinyl to 1-acenaphthenyl. In addition, a transition state allowing the direct isomerization between 3-H-acenaphthylenyl (A2R5H) and 1-acenaphthenyl (HA2R5) was identified in the present work, and the corresponding kinetic data as well as those of subsequent hydrogen loss were deduced.

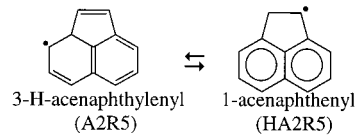

(34)

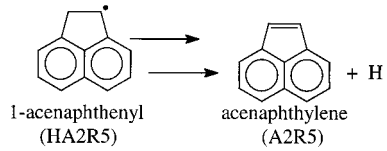

(35)

Another interesting result of the exploration of the potential surface is the formation of a four-membered ring species, A2R4. Similar to the formation of acenaphthylene (A2R5) it can be formed via either A2R4H or HA2R4 as the intermediate preceding hydrogen loss. In addition to their formation from 1-naphthylvinyl and 1-vinyl-2-naphthyl, also direct isomerization between both four-membered ring radicals has been shown to be possible.

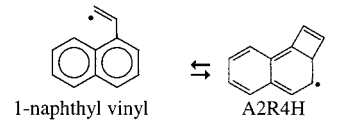

(36)

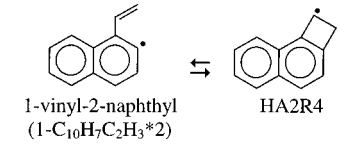

(37)

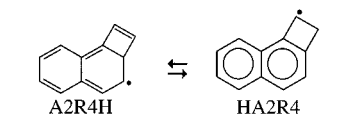

(38)

The rate constants of reactions 36−38 as well as their reverse reactions were determined by means of transition state theory. Finally, both four-membered rings containing radicals can yield the corresponding stable species via hydrogen loss.

The high-pressure-limit rate constant of reaction 39 has been determined in the present work while for reaction 40 the corresponding one determined for hydrogen loss of HA1R4 (11) has been used. The extremely high activation barrier of nearly 300 kJ mol^{-1} does not allow significant formation of A2R4, containing a four-membered ring.

TABLE 4: Inputs for Chemical Activation Analysis of 1-$C_{10}H_7$ + C_2H_2

parameter	used in present work
k_4 (cm^3 mol^{-1} s^{-1})	$(1.87 \times 10^7)T^{1.787}$ exp(−13.65 kJ/*RT*)
1-$C_{10}H_7$CHCH: mass (amu)	153.0
1-$C_{10}H_7$CHCH: σ (Å)	6.568[43]
1-$C_{10}H_7$CHCH: ϵ/k_b (K)	523.4[43]
Well 1: 1-$C_{10}H_7$CHCH	
→ 1-$C_{10}H_7$ + C_2H_2	$(4.11 \times 10^{10})T^{1.422}$ exp(−181 kJ/*RT*)
→ 1-$C_{10}H_7C_2H$ + H	$(2.10 \times 10^9)T^{1.560}$ exp(−158 kJ/*RT*)
→ A2R5H	$(1.35 \times 10^{10})T^{0.502}$ exp(−61 kJ/*RT*)
→ 1-$C_{10}H_7C_2H_3$*8	$(4.13 \times 10^9)T^{0.755}$ exp(−31 kJ/*RT*)
→ 1-$C_{10}H_7C_2H_3$*2	$(3.37 \times 10^9)T^{0.878}$ exp(−105 kJ/*RT*)
→ A2R4H	$(1.48 \times 10^{10})T^{0.571}$ exp(−124 kJ/*RT*)
Well 2: A2R5H	
→ 1-$C_{10}H_7$CHCH	$(1.20 \times 10^{11})T^{0.756}$ exp(−138 kJ/*RT*)
→ HA2R5	$(3.14 \times 10^{11})T^{0.479}$ exp(−65 kJ/*RT*)
A2R5 + H	$(6.21 \times 10^9)T^{1.269}$ exp(−113 kJ/*RT*)
Well 3: HA2R5	
→ 1-$C_{10}H_7C_2H_3$*8	$(9.68 \times 10^{10})T^{0.852}$ exp(−215 kJ/*RT*)
→ A2R5H	$(1.34 \times 10^{11})T^{0.641}$ exp(−162 kJ/*RT*)
→ A2R5 + H	$(2.07 \times 10^9)T^{1.579}$ exp(−193 kJ/*RT*)
Well 4: 1-$C_{10}H_7C_2H_3$ × 8	
→ 1-$C_{10}H_7$CHCH	$(1.22 \times 10^9)T^{0.915}$ exp(−33 kJ/*RT*)
→ HA2R5	$(7.53 \times 10^9)T^{0.595}$ exp(−43 kJ/*RT*)
Well 5: 1-$C_{10}H_7C_2H_3$ × 2	
→ 1-$C_{10}H_7$CHCH	$(1.22 \times 10^9)T^{0.989}$ exp(−101 kJ/*RT*)
→ HA2R4	$(6.98 \times 10^9)T^{0.682}$ exp(−114 kJ/*RT*)
Well 6: A2R4H	
→ 1-$C_{10}H_7$CHCH	$(3.08 \times 10^{11})T^{0.515}$ exp(−82 kJ/*RT*)
→ HA2R4	$(1.17 \times 10^{11})T^{0.646}$ exp(−167 kJ/*RT*)
→ A2R4 + H	$(1.11 \times 10^9)T^{1.649}$ exp(−214 kJ/*RT*)
Well 7: HA2R4	
→ 1-$C_{10}H_7$C2H3 × 2	$(2.10 \times 10^{11})T^{0.670}$ exp(−162 kJ/*RT*)
→ A2R4H	$(6.07 \times 10^{10})T^{0.796}$ exp(−252 kJ/*RT*)
→ A2R4 + H	$(3.14 \times 10^7)T^{2.386}$ exp(−295 kJ/*RT*)[a]
argon (bath gas): mass (amu)	40.0
argon: σ (Å), ϵ/k (K), $\langle \Delta E \rangle$ (J mol^{-1})	3.33, 136.5, 2636[30]

[a] Assumed same as determined for A1R4H → A1R4 + H

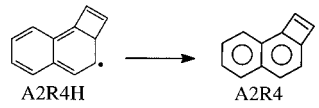

(39)

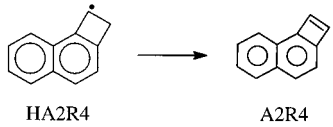

(40)

On the basis of this potential surface and the corresponding kinetic data a chemical-activation analysis using the CHEMDIS software[31] was performed in order to determine the apparent rate constants $k(T,P)$ of reactions leading to the various stable and unstable species. The input parameters for the CHEMDIS computation are summarized in Table 4. The rate constants of the different reaction channels are given for all wells, i.e., the chemically activated complex resulting from acetylene addition to 1-naphthyl and the subsequent isomerization products. Three representative frequencies for each species are calculated from the heat capacities[34] given in Table 1. Uncertainties in the branching ratios between the formation of 1-naphthylvinyl, 1-naphthylacetylene, and acenaphthylene, i.e., between reactions 3, 4, and 5, are assessed and shown, by means of error bars, in Figure 5a−d. For this purpose, upper and lower values of the

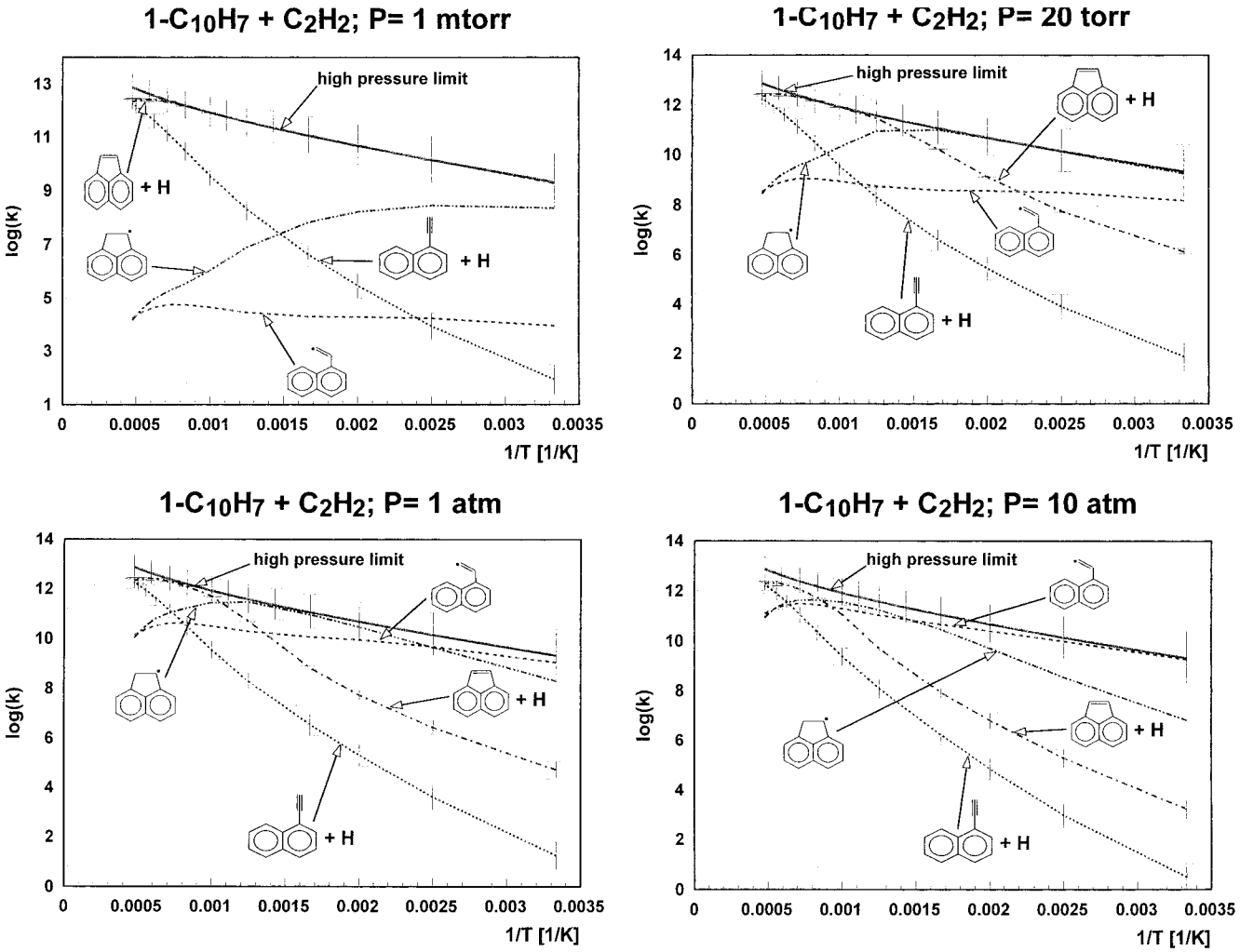

Figure 5. Computed rates for the reaction 1-$C_{10}H_7$ + C_2H_2 to form various products: —, high-pressure limit; ---, apparent rate constant of 1-$C_{10}H_7$ + C_2H_2 → 1-$C_{10}H_7$CHCH; ▪▪▪, apparent rate constant of 1-$C_{10}H_7$ + C_2H_2 → 1-$C_{10}H_7C_2H$ + H; •—•—, apparent rate constant of 1-$C_{10}H_7$ + C_2H_2 → acenaphthylene + H ▪▪—▪▪—, apparent rate constant of 1-$C_{10}H_7$ + C_2H_2 → HA2R5. (a) P = 1 mTorr, (b) P= 20 Torr, (c) P = 1 atm, (d) P = 10 atm.

ring closure rate and its reverse reaction 29, as well as of hydrogen loss to 1-naphthylacetylene (28), have been defined by simultaneous variation of the activation energies by ±4 kJ/mol and of the frequencies by ±15 cm^{-1}.

The results of the chemical activation analysis show a strong pressure and temperature dependence of the relative importance of the different reaction pathways and are shown in Figure 5a−d. Branching ratios for the major products are shown in Figure 6. Rate constants at 20 and 40 Torr as well at 1 and 10 atm are summarized in Table 5 for the temperature range from 300 to 2100 K. The high-pressure limit rate constant for reaction 26 is given, including uncertainties determined by means of the same approach as discussed above. Uncertainties in the rate of the entrance channel (26), very similar to reaction 12, which has been discussed above, do not significantly affect the branching ratio between reactions 3, 4, and 5 and are therefore not taken into account in the subsequent uncertainty analysis.

The formation of the stabilized initial adduct 1-naphthylvinyl (1-$C_{10}H_7$CHCH) shows only a slight dependence on temperature but increases significantly with pressure. Uncertainties of the rate constants of reaction 4 based on the lower and upper limits of hydrogen loss and ring closure reactions are less than 15% and are omitted for clarity. On the basis of the absolute and in particular the relative rate constant of its formation from 1-naphthyl and acetylene compared to the competing channels, 1-naphthylvinyl may play a significant role at high pressure as an intermediate in the growth process to phenanthrene ($C_{14}H_{10}$). The formation of acenaphthylene after ring closure to a five-membered ring represents under low-pressure conditions, i.e., below 40 Torr, the most important reaction, at least for temperatures above 500 K. Comparison of the two acenaphthylene formation pathways through 3-H-acenaphthylenyl (A2R5H) and 1-acenaphthenyl (HA2R5) shows a significantly higher contribution of the latter one, except at low temperatures and high pressures, i.e., under conditions of small absolute rates. Pressure increase leads to a more significant contribution of the pathway forming 1-naphthylacetylene. This more pronounced domination of acenaphthylene formation at high temperature and low pressure is consistent with the observation of higher fullerene yields under those conditions.[51] As a matter of fact, fullerene formation requires the formation of five-membered rings while the formation of arylacetylene represents the first step in a reaction sequence leading to an additional hexagon. The formation of the four-membered ring species A2R4 is from both thermodynamic and kinetic points of view insignificant and can be therefore excluded as an intermediate in combustion processes. Similar to acetylene addition to phenyl, the apparent rate constants of the formation of the four-membered ring radical A2R4H and HA2R4 (Figure 1) exhibit a maximum which is shifting to higher temperatures with

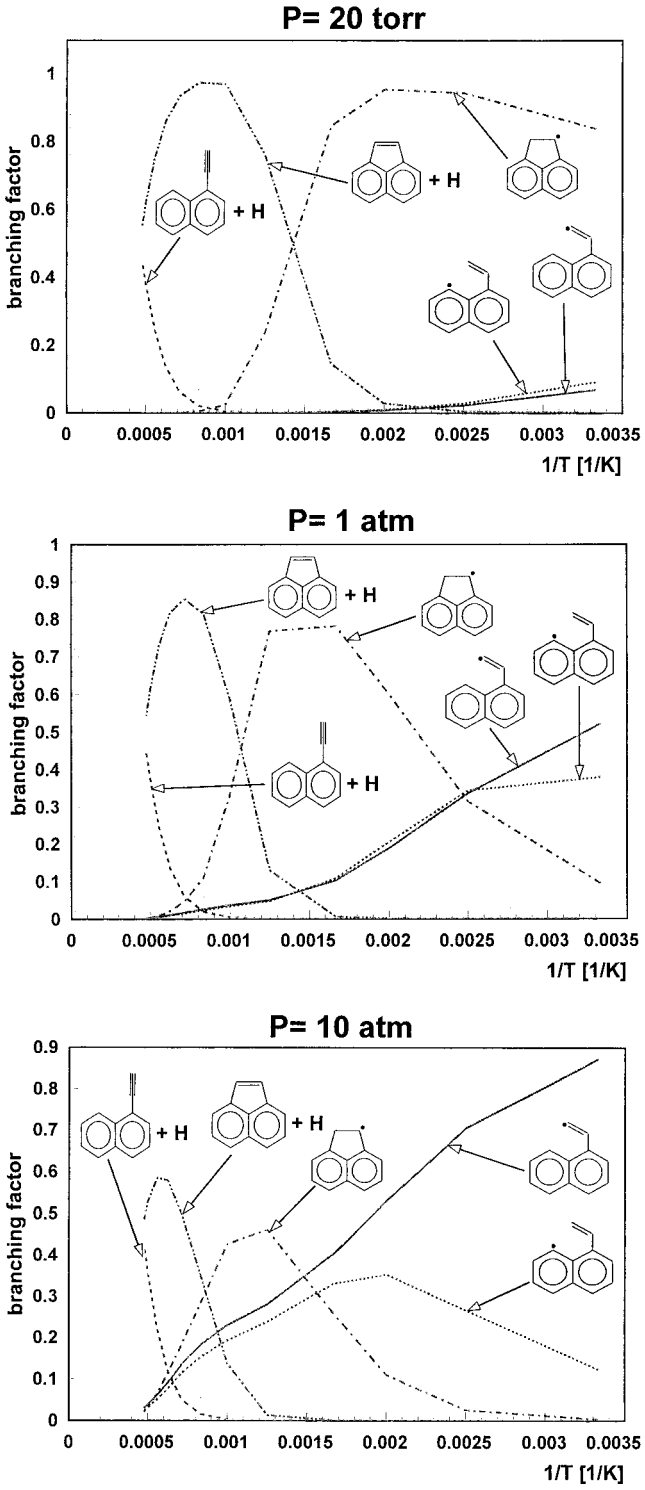

Figure 6. Computed branching ratios for the major products from the reaction 1-$C_{10}H_7$ + C_2H_2: (a) $P = 20$ Torr, (b) $P = 1$ atm, (c) $P = 10$ atm.

increasing pressures. The absolute value of the maximum is increasing simultaneously but remains below that of the competing pathways. In conclusion, A2R4H and HA2R4 can be considered as negligible for acetylene addition to 1-naphthyl.

Formation of 1-vinyl-2-naphthyl by acetylene addition to 1-naphthyl is significantly slower than reaction 4 leading to 1-naphthylvinyl and therefore plays no role under the pressure and temperature conditions investigated in the present work. Absolute values as well as pressure and temperature dependences of 1-vinyl-8-naphthyl formation are very similar to those

TABLE 5: Computed Rate Constants for 1-$C_{10}H_7$ + C_2H_2 → 1-$C_{10}H_7CHCH$, 1-$C_{10}H_7C_2H_3$*8, 1-$C_{10}H_7C_2H$ + H, HA2R5 and A2R5 + H between 300 and 2100 K at 20 and 40 Torr, 1 and 10 atm

reaction	$k_{20\text{Torr}}$ ($cm^3\ mol^{-1}\ s^{-1}$)	$k_{40\text{Torr}}$ ($cm^3\ mol^{-1}\ s^{-1}$)	$k_{1\text{atm}}$ ($cm^3\ mol^{-1}\ s^{-1}$)	$k_{10\text{atm}}$ ($cm^3\ mol^{-1}\ s^{-1}$)
→ 1-$C_{10}H_7CHCH$	$(1.2 \times 10^{14})T^{-1.52}$ exp(−13 kJ/*RT*)	$(5.1 \times 10^{14})T^{-1.61}$ exp(−14 kJ/*RT*)	$(4.5 \times 10^{18})T^{-2.35}$ exp(−22 kJ/*RT*)	$(2.9 \times 10^{18})T^{-1.97}$ exp(−25 kJ/*RT*)
→ 1-$C_{10}H_7C_2H_3$*8	$(3.6 \times 10^{14})T^{-1.69}$ exp(−12 kJ/*RT*)	$(1.7 \times 10^{15})T^{-1.79}$ exp(−13 kJ/*RT*)	$(4.3 \times 10^{20})T^{-2.96}$ exp(−25 kJ/*RT*)	$(2.8 \times 10^{23})T^{-3.42}$ exp(−38 kJ/*RT*)
→ 1-$C_{10}H_7C_2H$ + H	$(9.6 \times 10^{-9})T^{6.44}$ exp(−36 kJ/*RT*)	$(1.7 \times 10^{-8})T^{6.37}$ exp(−37 kJ/*RT*)	$(9.9 \times 10^{-6})T^{5.59}$ exp(−45 kJ/*RT*)	$(1.1 \times 10^{-5})T^{5.61}$ exp(−50 kJ/*RT*)
→ HA2R5	$(7.7 \times 10^{45})T^{-10.85}$ exp(−56 kJ/*RT*)	$(1.9 \times 10^{45})T^{-10.56}$ exp(−58 kJ/*RT*)	$(4.6 \times 10^{41})T^{-9.00}$ exp(−65 kJ/*RT*)	$(9.8 \times 10^{34})T^{-6.67}$ exp(−68 kJ/*RT*)
→ A2R5 + H	$(3.6 \times 10^{24})T^{-3.18}$ exp(−62 kJ/*RT*)	$(5.6 \times 10^{23})T^{-2.92}$ exp(−63 kJ/*RT*)	$(2.3 \times 10^{17})T^{-0.98}$ exp(−61 kJ/*RT*)	$(3.5 \times 10^{10})T^{1.07}$ exp(−59 kJ/*RT*)

of 1-naphthylvinyl, i.e., exhibit a maximum which shifts to higher temperatures with increasing pressure. 1-Vinyl-8-naphthyl might contribute as an intermediate to PAH growth, in particular above atmospheric pressure; three-parameter fits of the corresponding rate constants are included in Table 5.

Other interesting results are the apparent rate constants of the formation of 3-H-acenaphthylenyl (A2R5H) and 1-acenaphthenyl (HA2R5), two precursors of acenaphthylene prior to hydrogen loss.

$$1\text{-}C_{10}H_7 + C_2H_2 \rightarrow A2R5H \quad (41)$$

The maxima of both rate constants increase significantly with

$$1\text{-}C_{10}H_7 + C_2H_2 \rightarrow HA2R5 \quad (42)$$

pressure, but only the formation of 1-acenaphthenyl is fast enough to compete with the other pathways. Formation of 3-H-acenaphthylenyl depends only slightly on temperature and shows maxima between about 4×10^4 cm^3 mol^{-}1 s^{-1} at 1 mTorr and about 10^{10} cm^3 mol^{-1} s^{-1} at 10 atm. The rate constants of 1-acenaphthenyl (HA2R5) formation are plotted in Figure 5a−d and three-parameter fits are given in Table 5. 1-Acenaphthenyl could be present in detectable concentrations in certain flame environments and its experimental identification, e.g. by means of the radical scavenging technique,[52,53] would allow validation of the rate constant deduced in the present work.

IV. Conclusions

Rate constants of reactions believed to be essential for the formation of PAHs containing two and three rings were calculated by means of ab initio computational techniques without any parameter adjustments. The potential surfaces of the reactions $C_6H_5 + C_2H_2$ and $1\text{-}C_{10}H_7 + C_2H_2$ were explored using isodesmic BLYP/DZVP calculations and the B3LYP/cc-pVDZ method. These were checked versus ROMP2 calculations. Transition states were determined and rate constants obtained by means of transition state theory. Apparent rate constants leading to the different species present on the potential surface were obtained after a chemical activation analysis for different pressures. The comparison of the predicted rate constants with literature experimental data for the reaction $C_6H_5 + C_2H_2$ available for different temperatures and pressures allowed the validation of the chosen approach. The computed rate constants were within a factor of 4 of the experimental ones measured at temperatures between room temperature and about 1400 K; therefore, the techniques used in the present work should be a powerful tool for the systematic prediction of a large range of rate constants relevant in combustion chemistry as well as of their pressure dependence.

The exploration of the potential energy surfaces of the addition of acetylene to phenyl and 1-naphthyl revealed interesting features such as the presence of four-membered-ring containing species and internal intramolecular hydrogen-abstractions. The chemical activation analysis showed that the formation of acenaphthylene is favored at low pressure. This finding is consistent with the experimental observation of higher yields of fullerenes under such conditions, since this type of reaction is an important route to polycyclic aromatic hydrocarbons containing five-membered rings. The stabilized initial adduct, 1-naphthylvinyl, may play a role in the growth process of PAHs at pressures above 1 atm. The rate constant for 1-acenaphthenyl formation is surprisingly high and exhibits a maximum which shifts to higher and higher temperature with increasing pressure. The detection of 1-acenaphthenyl by radical scavenging seems to be possible and will be attempted in ongoing work. The extension of the present study to the reactions between acetylene and PAH radicals larger than 1-naphthyl will give a deeper insight in the trends of absolute but also relative rate constants, in particular concerning the competition between the formation of five- and six-membered rings, in the growth process to larger and larger PAHs, leading ultimately to high molecular weight soot precursors and fullerenes. The relatively large C_{12} systems studied here are far from the high-pressure-limit, indicating that chemical activation effects may be important even for larger PAHs. Uncertainties in the ab initio high-pressure-limit rate constants of the elementary reaction steps used as inputs to the chemical-activation analysis do not change the qualitative conclusions but limit the quantitative accuracy of the computed rates $k(T,P)$.

To summarize, under sooting flame conditions, the dominant product from the addition of 1-naphthyl radical to acetylene is acenaphthylene. At very high temperatures ($T > 2000$ K), 1-naphthylacetylene becomes comparably important. As the temperature is lowered below 1000 K, the 1-acenaphthenyl radical becomes the dominant product in the pressure range relevant for combustion. At very high pressures and low temperatures, the initial adduct 1-naphthylvinyl radical and its isomer 1-vinyl-8-naphthyl become the major reaction products.

Note Added in Proof. Potential energy surfaces for C_2H_2 addition to many PAH radicals including 1-naphthyl have been determined recently by Marsh and Wornat[54] using corrected semi-empirical calculations.

Acknowledgment. We are grateful to the Division of Chemical Sciences, Office of Basic Energy Sciences, Office of Energy Research, U.S. Department of Energy, for financial support of this research under Grants No. DE-FG02-84ER13282 and 98ER14914. We also gratefully acknowledge additional financial support from ABB Alstom Power and from the EPA Center for Airborne Organics (Grant R824970-01-0). This work was partially supported by the National Computational Science Alliance under grants CHE000029N and CHE000004N and utilized the NCSA SGI/CRAY Origin2000 and NCSA HP/Convex Exemplar SPP-2000.

Supporting Information Available: B3LYP minima and the corresponding transition states. This material is available free of charge via the Internet at http://pubs.acs.org.

References and Notes

(1) Durant, J. L.; Busby, W. F.; Lafleur, A. L.; Penman, B. W.; Crespi, C. L. *Mutat. Res.* **1996**, *371*, 123.

(2) Denissenko, M. F.; Pao, A.; Tang, M.; Pfeifer, G. P. *Science* **1996**, *274*, 430.

(3) Allen, J. O.; Dookeran, N. M.; Smith, K. A.; Sarofim, A. F.; Taghizadeh, K.; Lafleur, A. L. *Environ. Sci. Technol*. **1996**, *30*, 1023.

(4) Lafleur, A. L.; Howard, J. B.; Plummer, E.; Taghizadeh, K.; Necula, A.; Scott, L. T.; Swallow, K. C. *Polycycl. Aromatic Compds.* **1998**, *12*, 223.

(5) Pope, C. J.; Marr, J. A.; Howard, J. B. *J. Phys. Chem*. **1993**, *97*, 11001.

(6) Richter, H.; Grieco, W. J.; Howard, J. B. *Combust. Flame* **1999**, *119*, 1.

(7) Marinov, N. M.; Pitz, W. J.; Westbrook, C. K.; Castaldi, M. J.; Senkan, S. M. *Combust. Sci. Technol.* **1996**, *116*, 211−287.

(8) Bittner, J. D.; Howard, J. B. *Proc. Combust. Inst*. **1981**, *18*, 1105.

(9) Bockhorn, H.; Fetting, F.; Wenz, H. W. *Ber. Bunsen-Ges. Phys. Chem*. **1983**, *97*, 1067.

(10) Frenklach, M.; Clary, D. W.; Gardiner, W. C.; Stein, S. E. *Proc. Combust. Inst.* **1984**, *20*, 887.

(11) Johnston, H. S. *Gas-Phase Reaction Rate Theory*; Ronald Press: New York, 1966.

(12) Stein, S. E.; Fahr, A. *J. Phys. Chem*. **1985**, *89*, 3714.
(13) Alberty, R. A. *J. Phys. Chem*. **1989**, *93*, 3299.
(14) Alberty, R. A. *Proc. Combust. Inst*. **1990**, *23*, 487.
(15) Kiefer, J. H.; Mizerka, L. J.; Patel, M. R.; Wei, H.-C. *J. Phys. Chem*. **1985**, *89*, 2013.
(16) Madronich, S.; Felder, W. *J. Phys. Chem*. **1985**, *89*, 3556.
(17) Mebel, A. M.; Lin, M. C.; Yu, T.; Morokuma, K. *J. Phys. Chem. A* **1997**, *101*, 3189.
(18) Cioslowski, J.; Liu, G.; Martinov, M.; Piskorz, P.; Moncrieff, D. *J. Am. Chem. Soc.* **1996**, *118*, 5261.
(19) Fahr, A.; Stein, S. E. *Proc. Combust. Inst.* **1988**, *22*, 1023.
(20) Heckmann, E.; Hippler, H.; Troe, J. *Proc. Combust. Inst.* **1996**, *26*, 543.
(21) Yu, T.; Lin, M. C.; Melius, C. F. *Int. J. Chem. Kinet*. **1994**, *26*, 1095.
(22) Cioslowski, J.; Schimeczek, M.; Piskorz, P.; Moncrieff, D. *J. Am. Chem. Soc*. **1999**, *121*, 3773.
(23) Grieco, W. J.; Lafleur, A. L.; Swallow, K. C.; Richter, H.; Taghizadeh, K.; Howard, J. B. *Proc. Combust. Inst.* **1998**, *27*, 1669.
(24) Lafleur, A. L.; Taghizadeh, K.; Howard, J. B.; Anacleto, J. F.; Quilliam, M. A. *J. Am. Soc. Mass Spectrom*. **1996**, *7*, 276.
(25) Wang, H.; Frenklach, M. *J. Phys. Chem*. **1994**, *98*, 11465.
(26) Wang, H.; Frenklach, M. *Combust. Flame* **1997**, *110*, 173.
(27) Dean, A. M. *J. Phys. Chem*. **1985**, *89*, 4600.
(28) Westmoreland, P. R.; Howard, J. B.; Longwell, J. P.; Dean, A. M. *AIChE J*. **1986**, *32*, 1971.
(29) Westmoreland, P. R.; Dean, A. M.; Howard, J. B.; Longwell, J. P. *J. Phys. Chem*. **1989**, *93*, 8171.
(30) Dean, A. M.; Bozzelli, J. W.; Ritter, E. R. *Combust. Sci. Technol*. **1991**, *80*, 63.
(31) Chang, A. Y.; Bozzelli, J. W.; Dean, A. M., *Z. Phys. Chem.*, in press.
(32) Troe, J. *J. Chem. Phys*. **1977**, *66*, 4745.
(33) Gilbert, R. G.; Luther, K.; Troe, J. *Ber. Bunsen-Ges. Phys. Chem*. **1983**, *87*, 169.
(34) Bozzelli, J. W.; Chang, A. Y.; Dean, A. M. *Int. J. Chem. Kinet.* **1997**, *29*, 161.
(35) Forst, W. *J. Phys. Chem.* **1982**, *86*, 1771.
(36) Andzelm, J.; Wimmer, E. *J. Chem. Phys.* **1992**, *96*, 1280.
(37) UniChem, Oxford Molecular Group PLC: Beaverton, OR 1997.
(38) Becke, A. D. *Phys. Rev. A* **1988**, *38*, 3098.
(39) Lee C.; Yang W.; Parr R. G. *Phys. Rev. B.* **1998**, *37*, 785.
(40) Godbout, N.; Andzelm, J.; Wimmer E.; Salahub, D. R. *Can. J. Chem*. **1992**, *70*, 560.
(41) Mallard, W. G., Linstrom, P. J., Eds.; NIST Chemistry WebBook, NIST Standard Reference Database Number 69, February 2000, National Institute of Standards and Technology, Gaithersburg, MD 20899 (http://webbook.nist.gov)
(42) Ritter, E. R.; Bozzelli, J. W. *Int. J. Chem. Kinet.* **1991**, *23*, 767.
(43) Frisch, M. J.; Trucks, G. W.; Schlegel, H. B.; Scuseria, G. E.; Robb, M. A.; Cheeseman, J. R.; Zakrzewski, V. G.; Montgomery, J. A., Jr.; Stratmann, R. E.; Burant, J. C.; Dapprich, S.; Millam, J. M.; Daniels, A. D.; Kudin, K. N.; Strain, M. C.; Farkas, O.; Tomasi, J.; Barone, V.; Cossi, M.; Cammi, R.; Mennucci, B.; Pomelli, C.; Adamo, C.; Clifford, S.; Ochterski, J.; Petersson, G. A.; Ayala, P. Y.; Cui, Q.; Morokuma, K.; Malick, D. K.; Rabuck, A. D.; Raghavachari, K.; Foresman, J. B.; Cioslowski, J.; Ortiz, J. V.; Baboul, A. G.; Stefanov, B. B.; Liu, G.; Liashenko, A.; Piskorz, P.; Komaromi, I.; Gomperts, R.; Martin, R. L.; Fox, D. J.; Keith, T. A.; Al-Laham, M. A.; Peng, C. Y.; Nanayakkara, A.; Gonzalez, C.; Challacombe, M.; Gill, P. M. W.; Johnson, B. G.; Chen, W.; Wong, M. W.; Andres, J. L.; Head-Gordon, M.; Replogle, E. S.; Pople, J. A. *Gaussian 98*, Rev. A.7, Gaussian, Inc.: Pittsburgh, PA, 1998.
(44) Woon, D. E.; Dunning, T. H., Jr. *J. Chem. Phys*. **1993**, *98*, 1358.
(45) Scott, A. P. Radom, L. *J. Phys. Chem*. **1996**, *100*, 16502.
(46) Becke, A. M. *J. Chem. Phys*. **1993**, *98*, 5648.
(47) Knowles, P. J.; Andrews, J. S.; Amos, R. D.; Handy, N. C.; Pople, J. A. *Chem. Phys. Lett.* **1991**, *186*, 130.
(48) (a) Frenklach, M.; Clary, D. W.; Gardiner, W. C.; Stein, S. E. *Proc. Combust. Inst*. **1986**, *21*, 1067. (b) Frenklach, M.; Moriarty, N. W.; Brown, N. J. *Proc. Combust. Inst.* **1998**, *27*, 1655.
(49) Yu, T.; Lin, M. C. *J. Am. Chem. Soc*. **1993**, *115*, 4371.
(50) Pope, C. J.; M.S. Thesis, Department of Chemical Engineering, Massachusetts Institute of Technology 1988, Cambridge, MA.
(51) Howard, J. B.; Lafleur, A. L.; Makarovsky, Y.; Mitra, S.; Pope, C. J.; Yadav, T. K. *Carbon* **1992**, *30*, 1183.
(52) Hausmann, M.; Hebgen, P.; Homann, K.-H. *Proc. Combust. Inst*. **1992**, *24*, 793.
(53) Benish, T. G. PAH Radical Scavenging in Fuel-Rich Premixed Benzene Flames. Ph.D. Thesis, Massachusetts Institute of Technology, Cambridge, MA, 1999.
(54) Marsh, N. D.; Wornat, M. J. *Proc. Combust. Inst.* **2000**, *28*, in press.